Kinetic theory of low-frequency Alfvén modes in tokamaks

To cite this article: Fulvio Zonca *et al* 1996 *Plasma Phys. Control. Fusion* **38** 2011

View the article online for updates and enhancements.

Related content

- Existence of discrete modes in an unstable shear Alfvén continuous spectrum
  Fulvio Zonca, Liu Chen, Robert A Santoro et al.

- Structures of low-frequency shear Alfvén continuum
  Ilija Chavdarovski and Fulvio Zonca

- High and low frequency Alfvén modes in tokamaks
  S. Briguglio, L. Chen, Jiaqi Dong et al.

Recent citations

- The residual zonal flow in tokamak plasmas with a poloidal electric field
  Wenjia WANG *et al*

- Theoretical studies and simulations of mode structure symmetry breaking in tokamak plasmas in the presence of energetic particles
  Z X Lu *et al*

- Turbulent generation of poloidal asymmetries of the electric potential in a tokamak
  P Donnel *et al*

Kinetic theory of low-frequency Alfvén modes in tokamaks

Fulvio Zonca†, Liu Chen and Robert A Santoro

Department of Physics and Astronomy, University of California, Irvine, CA 92717-4575, USA

Abstract. The kinetic theory of low-frequency Alfvén modes in tokamaks is presented. The inclusion of both diamagnetic effects and finite core-plasma ion compressibility generalizes previous theoretical analyses (Tsai S T and Chen L 1993 *Phys. Fluids* B **5** 3284) of kinetic ballooning modes and clarifies their strong connection to beta-induced Alfvén eigenmodes. The derivation of an analytic mode dispersion relation allows us to study the linear stability of both types of modes as a function of the parameters characterizing the local plasma equilibrium and to demonstrate that the most unstable regime corresponds to a strong coupling between the two branches due to the finite thermal ion temperature gradient. In addition, we also show that, under certain circumstances, non-collective modes may be present in the plasma, formed as a superposition of local oscillations which are quasi-exponentially growing in time.

1. Introduction

The experimental observation [1] of large energetic ion losses due to Alfvén waves with frequencies lower than that of the toroidal Alfvén eigenmode (TAE) [2] has recently demonstrated that low-frequency Alfvén waves can be as deleterious as TAE modes to energetic particle confinement. Experimentally, these modes have the predominant polarization of shear Alfvén waves [1] and they have been given the name of beta-induced Alfvén eigenmodes (BAE) [3] since their frequency is located in the low-frequency beta-induced gap in the shear Alfvén continuous spectrum [4], which is caused by finite plasma compressibility.

Ideal magneto-hydrodynamic (MHD) theories predict the beta-induced frequency gap at [3] $0 < (\omega/\omega_A)^2 \lesssim \gamma\beta q^2$, where ω is the mode frequency, γ is the ratio of specific heats, β the ratio of kinetic and magnetic pressures, q the safety factor, $\omega_A = v_A/qR_0$ the Alfvén frequency, R_0 the major radius of the toroidal plasma column, $v_A = B/\sqrt{4\pi\varrho}$ the Alfvén speed and ϱ the plasma mass density. This fact, along with the experimental observation that BAEs are shear Alfvén waves with frequency within or near the beta-induced gap, indicates that these modes have long parallel (to the equilibrium magnetic field $\boldsymbol{B}$) wavelengths, i.e. $\omega \simeq k_\parallel v_A \approx \sqrt{\gamma\beta}v_A/R_0 \rightarrow k_\parallel \approx \sqrt{\gamma\beta}/R_0$ ($k_\parallel$ being the parallel wavevector), and that the relevant BAE frequency range is ordered as the thermal ion transit frequency, $\omega \approx \omega_{ti} = \sqrt{2T_i/m_i}/qR_0$ (T_i is the ion temperature in energy units and m_i the ion mass). Furthermore, there is clear experimental evidence [1] that diamagnetic effects are important for the BAE dynamics, since typically $\omega \approx \omega_{*pi} = (cT_i/e_i B^2)(\boldsymbol{k} \times \boldsymbol{B}) \cdot \nabla \ln P_i$, the core-plasma ion diamagnetic frequency. Here, e_i is the ion electric charge, P_i the ion pressure and $\boldsymbol{k}$ the wavevector.

---

† Permanent Address: Associazione EURATOM-ENEA sulla Fusione, CP 65-00044 Frascati, Rome, Italy.

From the previous discussion, it is evident that ideal MHD is inadequate to construct a realistic theory of BAE modes, for which $\omega \approx \omega_{\mathrm{ti}} \approx \omega_{*\mathrm{pi}}$, since finite core-plasma ion compressibility is expected to strongly affect the mode dynamics via resonant interactions with the ion transit motion along magnetic field lines. Moreover, it is important to clarify any relationship of BAEs with kinetic ballooning modes [5, 6] (KBM), which are expected to occur in the same frequency range. Previous theories of resonant excitations of KBM by energetic particles [5, 6] have shown that these modes, like BAEs, belong to the shear Alfvén branch and have $\omega \approx \omega_{*\mathrm{pi}}$. However, these theories assumed incompressible oscillations, thereby neglecting $\omega \approx \omega_{\mathrm{ti}}$ wave–particle resonances with core-plasma ions.

In the present paper we develop a unified theory for Alfvén waves belonging to the BAE/KBM branches by accounting for finite core-plasma compressibility and diamagnetic effects on the same footing. In this respect, we present the kinetic theory of high toroidal mode number [5, 6] low-frequency Alfvén modes in a high-β plasma ($\beta = \mathrm{O}(\epsilon)$; $\epsilon = a/R_0$, a being the plasma minor radius), which we may refer to as drift Alfvén kinetic ballooning modes. As a relevant and novel result we show that the most unstable scenario corresponds to the situation in which BAE and KBM are strongly coupled due to the presence of a finite temperature gradient of the thermal ions. The validity of the ideal MHD assumption of negligible parallel electric field perturbations ($\delta E_{\parallel} \simeq 0$) is also discussed, since, in general, the coupling between shear Alfvén and acoustic branches is not negligible at $\omega \approx \omega_{\mathrm{ti}} \approx \omega_{*\mathrm{pi}}$. More specifically, we show that, for long wavelength modes ($k_{\parallel} \approx \beta^{1/2}/R_0$), the $\delta E_{\parallel} \simeq 0$ assumption holds for waves propagating in the ion diamagnetic direction, whereas it may break down for modes propagating in the electron diamagnetic direction and/or modes with $\omega_{*\mathrm{pi}}/\omega = \mathrm{O}(1/\beta)$, which are strongly coupled to the slab-like ion temperature gradient (ITG) driven wave [7–9].

Since our goal is to study the BAE/KBM modes which may be resonantly excited by energetic ions, only the branches propagating in the ion diamagnetic direction are considered here. Nevertheless, in the present analysis we neglect the resonant excitation of the BAE/KBM branch by energetic particles. The primary reason for this choice is that of simplicity, which allows us to focus on the relevant features of the kinetic Alfvén spectrum due to the wave resonances with thermal ions. A second reason is that wave–particle resonances with core-plasma ions are important only in a narrow boundary layer (the *inertial layer*) centred at the mode rational surface, where the dynamics of energetic particles may be neglected [6] because of their large orbits (compared to the layer width). In this sense, the issue of the resonant excitation of BAE/KBM by energetic particles can be addressed by simply 'adding' the energetic particle dynamics to the present theory [6]. This problem will be analysed in a separate work.

The plan of the paper is as follows. In section 2 the theoretical model is presented and the relevant eigenmode equations are derived. Section 3 is devoted to a discussion of the characteristic two-scalelength mode structures of the Alfvén waves we wish to analyse. The knowledge of mode structures is used in section 4 to derive an analytic dispersion relation for BAE/KBM modes. The general features of BAE/KBM spectra are discussed in section 5, whereas detailed numerical studies of the analytic dispersion relation are presented in section 6. Section 7 gives final discussions and conclusions. An analysis of the $\delta E_{\parallel} \simeq 0$ ideal MHD assumption is presented in appendix A. Finally, appendix B provides an elementary derivation of the shear Alfvén continuous spectrum, with its modifications due to diamagnetic effects and core-plasma ion compressibility. There, a brief discussion of the relationship between singular mode structures and continuous spectra is also given.

2. Theoretical model and eigenmode equations

We consider a large aspect-ratio axisymmetric toroidal plasma equilibrium with shifted circular magnetic flux surfaces and with major and minor radii given by R_0 and a. For the sake of simplicity, we assume a high-β ($\beta = 8\pi P/B^2 \approx \epsilon = a/R_0$, P being the total core-plasma pressure and B the equilibrium magnetic field) (s, α) model equilibrium [10], which is entirely determined by the local equilibrium parameters s, the magnetic shear, and $\alpha = -R_0 q^2 \beta'$. We also concentrate on waves with high toroidal mode numbers, such that $k_\vartheta \rho_{\mathrm{Li}} \approx \epsilon$ (k_ϑ being the poloidal component of the wavevector $\boldsymbol{k}$ and ρ_{Li} the ion Larmor radius). This assumption does not cause any loss of generality, since this is the range of most unstable mode numbers [6].

As usual [11, 12], we will describe the plasma oscillations in terms of three fluctuating scalar fields: the scalar potential perturbation $\delta\phi$; the parallel (to $\boldsymbol{b} = \boldsymbol{B}/B$) magnetic field perturbation $\delta B_\parallel$; and the perturbed field $\delta\psi$, related to the parallel vector potential fluctuation $\delta A_\parallel$ by

$$\delta A_\parallel \equiv -\mathrm{i} \left(\frac{c}{\omega}\right) \boldsymbol{b} \cdot \nabla \delta\psi.$$

With this representation, the parallel electric field fluctuation is $\delta E_\parallel = -\boldsymbol{b} \cdot \nabla(\delta\phi - \delta\psi)$, and the ideal magneto-hydrodynamic (MHD) limit, $\delta E_\parallel = 0$, is obtained for $\delta\psi = \delta\phi$. Isolating adiabatic and convective particle responses to the wave, the perturbed particle distribution function can be expressed as [11, 12]

$$\delta f_s = \left(\frac{e}{m}\right)_s \left[\frac{\partial F_0}{\partial \mathcal{E}} \delta\phi - J_0(k_\perp \rho_{\mathrm{L}}) \frac{Q F_0}{\omega} \delta\psi \, \mathrm{e}^{\mathrm{i}L_k}\right]_s + \delta K_s \, \mathrm{e}^{\mathrm{i}L_{ks}} \tag{1}$$

where s is the species index, e_s the species electric charge, m_s the mass, F_{0s} the equilibrium distribution function, $\mathcal{E} = v^2/2$ the energy per unit mass, J_0 the Bessel function of zero index, $k_\perp$ the perpendicular (to $\boldsymbol{b}$) wavevector, $\rho_{\mathrm{L}s} = m_s c v_\perp / e_s B$ the Larmor radius, $Q F_{0s} = (\omega \partial_\mathcal{E} + \hat{\omega}_*)_s F_{0s}$, $\hat{\omega}_{*s} F_{0s} = (m_s c/e_s B)(\boldsymbol{k} \times \boldsymbol{b}) \cdot \nabla F_{0s}$, and $L_{ks} = (m_s c/e_s B)(\boldsymbol{k} \times \boldsymbol{b}) \cdot \boldsymbol{v}$.

Adopting the ballooning mode representation [10] in the space of the extended poloidal angle variable θ, the particle distribution function δK_s is derived from the gyrokinetic equation [12]

$$[\omega_{\mathrm{tr}} \partial_\theta - \mathrm{i}(\omega - \omega_{\mathrm{d}})]_s \, \delta K_s = \mathrm{i}\left(\frac{e}{m}\right)_s Q F_{0s}$$

$$\times \left[J_0(k_\perp \rho_{\mathrm{L}s})(\delta\phi - \delta\psi) + \left(\frac{\omega_{\mathrm{d}}}{\omega}\right)_s J_0(k_\perp \rho_{\mathrm{L}s})\delta\psi + \frac{v_\perp}{k_\perp c} J_1(k_\perp \rho_{\mathrm{L}s})\delta B_\parallel\right] \tag{2}$$

where $\omega_{\mathrm{tr}} = v_\parallel / qR$ is the transit frequency, $k_\perp^2 = k_\vartheta^2[1 + (s\theta - \alpha\sin\theta)^2]$ and $\omega_{\mathrm{d}s}$ is the magnetic drift frequency $\omega_{\mathrm{d}s}(\theta) = g(\theta) k_\vartheta m_s c(v_\perp^2/2 + v_\parallel^2)/e_s BR$, $g(\theta) = \cos\theta + [s\theta - \alpha\sin\theta]\sin\theta$. In the following, we will assume the electron response to be adiabatic, i.e. $\delta K_{\mathrm{e}} = 0$. Furthermore, it may be shown that, for the Alfvén modes we are interested in [12],

$$\delta B_\parallel = \frac{4\pi}{B^2}(\boldsymbol{k} \times \boldsymbol{b}) \cdot \nabla P \left(\frac{c}{\omega}\right)\delta\psi. \tag{3}$$

If we multiply both sides of equation (2) by $\mathrm{i}(4\pi \omega e_s J_0(k_\perp \rho_{\mathrm{L}s})/k_\vartheta^2 c^2)$ and then sum over the species index and integrate over the velocity space, it is well known that the following *vorticity* equation is obtained [5, 6]

$$B\boldsymbol{b} \cdot \nabla \left[\frac{1}{B} \frac{k_\perp^2}{k_\vartheta^2} \boldsymbol{b} \cdot \nabla \delta\psi \right] + \frac{\omega^2}{v_A^2} \left(1 - \frac{\omega_{*pi}}{\omega} \right) \frac{k_\perp^2}{k_\vartheta^2} \delta\phi$$

$$+ \frac{\alpha}{q^2 R^2} g(\theta) \delta\psi = \left\langle \sum_s \frac{4\pi e_s}{k_\vartheta^2 c^2} J_0(k_\perp \rho_{Ls}) \omega \omega_{ds} \delta K_s \right\rangle \tag{4}$$

where $\langle \ldots \rangle = \int \mathrm{d}\boldsymbol{v}(\ldots)$, $\omega_{*ps} = \omega_{*n_s} + \omega_{*T_s}$, $\omega_{*n_s} = (T_s c/e_s B)(\boldsymbol{k} \times \boldsymbol{b}) \cdot (\nabla n_s)/n_s$, $\omega_{*T_s} = (T_s c/e_s B)(\boldsymbol{k} \times \boldsymbol{b}) \cdot (\nabla T_s)/T_s$, n_s is the species particle density, T_s the temperature in energy units, and use has been made of the parallel Ampére's law

$$\frac{k_\perp^2}{k_\vartheta^2} \boldsymbol{b} \cdot \nabla \delta\psi = \frac{4\pi}{k_\vartheta^2 c^2} \mathrm{i}\omega \left\langle \sum_s e_s v_\parallel \delta f_s \right\rangle.$$

Equations (2)–(4), along with the *quasi-neutrality* condition, $\sum_s \langle e_s \delta f_s \rangle = 0$, form a closed set of integro-differential equations for the modes we are interested in, i.e. drift Alfvén kinetic ballooning modes. The quasi-neutrality equation can be put into the following form

$$\left(1 + \frac{1}{\tau} \right) (\delta\phi - \delta\psi) + \left(1 - \frac{\omega_{*pi}}{\omega} \right) b_i \delta\psi = \frac{T_i}{ne} \langle J_0(k_\perp \rho_{Li}) \delta K_i \rangle \tag{5}$$

where $\tau = T_e/T_i$, $b_i = k_\perp^2 (m_i c^2 T_i/e^2 B^2)$, $n = n_i = n_e$ and core-plasma ions with unit electric charge have been assumed.

3. Two-scale mode structures

Equations (2)–(5) describe a variety of drift Alfvén ballooning modes. They are in a complicated integro-differential form and little can be gleaned directly from these equations concerning the general properties of those waves. However, some analytic progress can be made and further insight can be gained when we recall the characteristic frequency and wavelength orderings assumed here; i.e. $\omega \approx \omega_{*pi} \approx \omega_{ti} \approx O(\beta^{1/2})\omega_A$ and $k_\vartheta \rho_{Li} \approx O(\beta)$.

3.1. Inertial layer physics: the large $|\theta|$ solution

It can be recognized that, at large $|\theta| = O(\beta^{-1/2})$, equations (2)–(5) always have a two-scale structure: in fact, the fluctuating fields vary on the short scale $\theta_0 \approx 1$ and on the long scale $\theta_1 \approx \beta^{-1/2}$. We consider this statement as an ansatz, to be self-consistently verified *a-posteriori*. Furthermore, for convenience, we work with new field quantities defined as follows: $\delta\Phi = (k_\perp/k_\vartheta)\delta\phi$, $\delta\Psi = (k_\perp/k_\vartheta)\delta\psi$ and $\delta\hat{B}_\parallel = (k_\perp/k_\vartheta)\delta B_\parallel$. Each field is thought to be expressed in terms of an asymptotic series in powers of $\beta^{1/2}$; e.g., $\delta\Phi = \delta\Phi^{(0)} + \delta\Phi^{(1)} + \delta\Phi^{(2)} + \cdots$, where $\delta\Phi^{(1)} = O(\beta^{1/2})$, $\delta\Phi^{(2)} = O(\beta)$, etc.

It is readily recognized that large $|\theta|$ values correspond, in real space, to a narrow toroidal layer centred around the mode rational surface, in ideal MHD usually referred to as the 'inertial layer'. At large $|\theta| = O(\beta^{-1/2})$, we have $k_\perp^2 \rho_{Li}^2 \approx b_i \approx (\omega_{di}/\omega)^2 \approx (\omega/\omega_A)^2 \approx \beta$. Equation (2), thus, gives

$$\delta K_i^{(0)} = - \left(\frac{e}{m_i} \right) \frac{Q F_{0i}}{\omega} \frac{k_\vartheta}{k_\perp} (\delta\Phi^{(0)} - \delta\Psi^{(0)})$$

which, substituted into the quasi-neutrality condition, equation (5), yields

$$\left(1 + \frac{1}{\tau} \right) (\delta\Phi^{(0)} - \delta\Psi^{(0)}) = \left(1 - \frac{\omega_{*n_i}}{\omega} \right) (\delta\Phi^{(0)} - \delta\Psi^{(0)})$$

i.e. $\delta\Psi^{(0)} = \delta\Phi^{(0)}$ to the lowest order. Thus, to the lowest order, equation (4) predicts that $\delta\Phi^{(0)} = \delta\Phi^{(0)}(\theta_1)$.

To the next $O(\beta^{1/2})$ order, equation (4) gives

$$\partial_{\theta_0}^2 \delta\Psi^{(1)} = -2\partial_{\theta_0}\partial_{\theta_1}\delta\Psi^{(0)} = 0$$

i.e. $\delta\Psi^{(1)} = 0$, since the θ_1 dependence of $\delta\Psi^{(1)}$ can be incorporated into $\delta\Psi^{(0)}$. Therefore, equation (2) reads

$$(\omega_{\text{tr}}\partial_{\theta_0} - i\omega)\delta K_i^{(1)} = -\omega_{\text{tr}}\partial_{\theta_1}\delta K_i^{(0)} + i\frac{k_\vartheta}{k_\perp}\left(\frac{e}{m_i}\right)QF_{0i}\left[\delta\Phi^{(1)} + \frac{\omega_{\text{di}}}{\omega}\delta\Phi^{(0)}\right]$$

which yields

$$\delta K_i^{(1)} = -i\frac{\omega_{\text{tr}}}{\omega}\partial_{\theta_1}\delta K_i^{(0)} + i\frac{k_\vartheta}{k_\perp}\frac{(e/m_i)QF_{0i}}{\omega^2 - \omega_{\text{tr}}^2}$$

$$\times \left\{\left[(i\omega + s\theta_1\omega_{\text{tr}})\frac{\omega_{\text{di}}(0)}{\omega}\delta\Phi^{(0)} + i\omega\delta\Phi_c^{(1)} + \omega_{\text{tr}}\delta\Phi_s^{(1)}\right]\cos\theta_0\right.$$

$$\left. + \left[(i\omega s\theta_1 - \omega_{\text{tr}})\frac{\omega_{\text{di}}(0)}{\omega}\delta\Phi^{(0)} + i\omega\delta\Phi_s^{(1)} - \omega_{\text{tr}}\delta\Phi_c^{(1)}\right]\sin\theta_0\right\} \quad (6)$$

where we have assumed

$$\delta\Phi^{(1)} = \delta\Phi_c^{(1)}(\theta_1)\cos\theta_0 + \delta\Phi_s^{(1)}(\theta_1)\sin\theta_0. \quad (7)$$

When substituted into the quasi-neutrality condition, equation (5), equation (6) yields

$$\left(1 + \frac{1}{\tau} + \left\langle\frac{T_i}{nm_i}QF_{0i}\frac{\omega}{\omega^2 - \omega_{\text{tr}}^2}\right\rangle\right)\delta\Phi^{(1)} = -\left\langle\frac{T_i}{nm_i}QF_{0i}\frac{\omega_{\text{di}}}{\omega^2 - \omega_{\text{tr}}^2}\right\rangle\delta\Phi^{(0)} \quad (8)$$

which gives

$$\delta\Phi_c^{(1)} = -\frac{2cT_i}{eB_0}\frac{k_\vartheta}{\omega R_0}\frac{N(\omega/\omega_{\text{ti}})}{D(\omega/\omega_{\text{ti}})}\delta\Phi^{(0)}$$

$$\delta\Phi_s^{(1)} = s\theta_1\delta\Phi_c^{(1)}. \quad (9)$$

Here, $\omega_{\text{ti}} = \sqrt{2T_i/m_i}/qR_0$ and the functions

$$N(x) = \left(1 - \frac{\omega_{*n_i}}{\omega}\right)[x + (1/2 + x^2)Z(x)] - \frac{\omega_{*T_i}}{\omega}[x(1/2 + x^2) + (1/4 + x^4)Z(x)]$$

$$D(x) = \left(\frac{1}{x}\right)\left(1 + \frac{1}{\tau}\right) + \left(1 - \frac{\omega_{*n_i}}{\omega}\right)Z(x) - \frac{\omega_{*T_i}}{\omega}[x + (x^2 - 1/2)Z(x)] \quad (10)$$

have been introduced, where $Z(x) = \pi^{-1/2}\int_{-\infty}^{\infty} e^{-y^2}/(y - x)\,dy$ is the plasma dispersion function. From equation (9), it is evident that our asymptotic expansion is consistent as long as $|D(\omega/\omega_{\text{ti}})| > O(\beta^{1/2})$. We assume that this is the case.

Proceeding further to the next $O(\beta)$ order, the vorticity equation, equation (4), becomes

$$\frac{\partial^2}{\partial\theta_0^2}\delta\Psi^{(2)} + \frac{\partial^2}{\partial\theta_1^2}\delta\Psi^{(0)} + \frac{\omega^2}{\omega_A^2}\left(1 - \frac{\omega_{*pi}}{\omega}\right)\delta\Phi^{(0)} = \frac{k_\vartheta}{k_\perp}\left\langle\frac{4\pi\omega e}{k_\vartheta^2 c^2}q^2 R_0^2\omega_{\text{di}}\delta K_i^{(1)}\right\rangle. \quad (11)$$

In order to avoid secularities of $\delta\Psi^{(2)}$ on the short θ_0 scale, equation (11) becomes

$$\frac{\partial^2}{\partial\theta_1^2}\delta\Psi^{(0)} + \frac{\omega^2}{\omega_A^2}\left(1 - \frac{\omega_{*pi}}{\omega}\right)\delta\Psi^{(0)} + q^2\frac{\omega\omega_{\text{ti}}}{\omega_A^2}$$

$$\times\left[\left(1 - \frac{\omega_{*n_i}}{\omega}\right)F(\omega/\omega_{\text{ti}}) - \frac{\omega_{*T_i}}{\omega}G(\omega/\omega_{\text{ti}}) - \frac{N^2(\omega/\omega_{\text{ti}})}{D(\omega/\omega_{\text{ti}})}\right]\delta\Psi^{(0)} = 0. \quad (12)$$

Here, the functions

$$F(x) = x(x^2 + \tfrac{3}{2}) + (x^4 + x^2 + \tfrac{1}{2})Z(x)$$
$$G(x) = x(x^4 + x^2 + 2) + (x^6 + x^4/2 + x^2 + \tfrac{3}{4})Z(x) \tag{13}$$

have been defined and use has been made of the fact that $\delta\Phi^{(0)} = \delta\Psi^{(0)}$ to lowest order. The determination of $\delta K_i^{(2)}$ and of $(\delta\Phi^{(0)} - \delta\Psi^{(0)})$ at $O(\beta)$ is not necessary for our present purposes. However, it is given in appendix A for completeness. Here, we just recall the result for the $O(\beta)$ quasi-neutrality equation, which is

$$\frac{\omega_{ti}^2}{2\omega^2}\left(1 - \frac{\omega_{*pi}}{\omega}\right)\frac{k_\perp}{k_\vartheta}\frac{\partial^2}{\partial\theta_i^2}\left[\frac{k_\vartheta}{k_\perp}(\delta\Phi^{(0)} - \delta\Psi^{(0)})\right] + \left(\frac{1}{\tau} + \frac{\omega_{*n_i}}{\omega}\right)(\delta\Phi^{(0)} - \delta\Psi^{(0)})$$
$$+ \left\{\left(1 - \frac{\omega_{*pi}}{\omega}\right)b_i + q^2 b_i \frac{\omega_{ti}}{\omega}\left[\left(1 - \frac{\omega_{*n_i}}{\omega}\right)F(\omega/\omega_{ti})\right.\right.$$
$$\left.\left. - \frac{\omega_{*T_i}}{\omega}G(\omega/\omega_{ti}) - \frac{N^2(\omega/\omega_{ti})}{D(\omega/\omega_{ti})}\right]\right\}\delta\Phi^{(0)} = \frac{b_i^{1/2}\alpha}{2^{3/2}q}\frac{\omega_{ti}}{\omega}\frac{k_\vartheta}{k_\perp}\left(1 - \frac{\omega_{*pi}}{\omega}\right)\delta\Psi^{(0)}.$$
$$\tag{14}$$

Equation (14) allows us to consider $\delta E_\parallel = 0$ for long wavelength modes propagating in the ion diamagnetic direction, such as those we are analysing in the present paper (cf introduction and appendix A). Therefore, equation (12) is the relevant eigenmode equation in the large $|\theta| = O(\beta^{-1/2})$ region. Incidentally, we note that a similar analysis of the inertial layer is presented in [13], where it was applied to the theory of resistive interchange ballooning modes.

3.2. Ideal region: the moderate $|\theta|$ solution

For moderate $|\theta| < O(\beta^{-1/2})$ values, equation (4) does not exhibit a two-scale structure any longer. The contribution of core-plasma inertia and core-plasma compressibility (i.e. the core-ion contribution to the angular brackets on the right-hand side) can be neglected, which is why this is usually referred to as the 'ideal region'. The vorticity equation, thus, becomes

$$\partial_\theta^2\delta\Psi^{(0)} - \frac{(s - \alpha\cos\theta)^2}{\left[1 + (s\theta - \alpha\sin\theta)^2\right]^2}\delta\Psi^{(0)} + \frac{\alpha\cos\theta}{\left[1 + (s\theta - \alpha\sin\theta)^2\right]}\delta\Psi^{(0)} = 0. \tag{15}$$

Equation (15) continuously matches onto equation (12) at large $|\theta|$, and, hence, these two equations define a well posed eigenvalue problem for the modes we wish to analyse. However, before proceeding further, it is worthwhile noting that it was possible to drop the core-ion inertia term in equation (15) since $(\omega^2/\omega_A^2) = O(\beta)$ *and* $\delta\Phi^{(0)} = \delta\Psi^{(0)}$ was assumed. As explained in appendix A, the latter assumption (which is the critical one) for modes with long parallel wavelength ($k_\parallel = O(\beta^{1/2}/qR_0)$) and $\omega_{*pi}/\omega = O(1)$ holds as long as $(1/\tau + \omega_{*n_i}/\omega) = O(1)$, e.g. for waves propagating in the ion diamagnetic direction. In the following, we assume that this is the case, so that considering $\delta\Phi^{(0)} = \delta\Psi^{(0)}$ is reasonable.

4. Dispersion relation

In the previous section, we have shown that, in the ideal region $|\theta| \sim \theta_0 \sim O(1)$, the vorticity equation is given by equation (15). Multiplying both its members by $\delta\Psi_{ID}^{(0)*}$ (here,

the subscript ID stands for 'ideal' solution), we may construct the following quadratic form [6]

$$\delta\Psi_{ID}^{(0)*}\partial_\theta\delta\Psi_{ID}^{(0)}|_{-\infty}^{+\infty} - 2\delta W_f = 0 \tag{16}$$

where δW_f is the ideal MHD contribution to the potential energy perturbation

$$\delta W_f = \frac{1}{2}\int_{-\infty}^{\infty} d\theta$$
$$\times \left[|\partial_\theta\delta\Psi_{ID}^{(0)}|^2 + \left(\frac{(s-\alpha\cos\theta)^2}{[1+(s\theta-\alpha\sin\theta)^2]^2} - \frac{\alpha\cos\theta}{[1+(s\theta-\alpha\sin\theta)^2]}\right)|\delta\Psi_{ID}^{(0)}|^2\right]. \tag{17}$$

In the large $|\theta|$ 'inertial' region, equation (12) is readily solved and gives

$$\delta\Psi_{IN}^{(0)} = \exp(i\Lambda|\theta_1|) \tag{18}$$

where the subscript IN stands for 'inertial' region solution and Λ is given by

$$\Lambda = \left\{\frac{\omega^2}{\omega_A^2}\left(1-\frac{\omega_{*pi}}{\omega}\right)+q^2\frac{\omega\omega_{ti}}{\omega_A^2}\left[\left(1-\frac{\omega_{*n_i}}{\omega}\right)F(\omega/\omega_{ti})-\frac{\omega_{*T_i}}{\omega}G(\omega/\omega_{ti})-\frac{N^2(\omega/\omega_{ti})}{D(\omega/\omega_{ti})}\right]\right\}^{1/2}. \tag{19}$$

Here, the square root in the expression for Λ is taken such that the *causality constraint*, Im $\Lambda > 0$, is satisfied. The asymptotic matching condition between $\delta\Psi_{IN}^{(0)}$ and $\delta\Psi_{ID}^{(0)}$ reads

$$\delta\Psi_{ID}^{(0)*}\partial_\theta\delta\Psi_{ID}^{(0)}|_{-\infty}^{+\infty} = 2\,i\Lambda. \tag{20}$$

Thus, equation (16) is equivalent to the following dispersion relation for drift Alfvén ballooning modes:

$$i\Lambda = \delta W_f. \tag{21}$$

In equation (21), δW_f is the same used in the MHD theory of ideal ballooning modes [10] and it may be evaluated by one of the well known numerical methods. Incidentally, we note that the inclusion of energetic particle dynamics in the present theory would lead to the dispersion relation of equation (21), with a contribution, δW_K, of energetic ions to the potential energy perturbation added on the right-hand side [6].

5. Relevant limits of the dispersion relation

A variety of Alfvén spectra are described by the dispersion relation equation (21), derived in the previous section. Specifically, the causality constraint Im $\Lambda > 0$ reduces to $\delta W_f < 0$, i.e. to the condition for ideal MHD instability. Since δW_f is purely real, Λ is purely imaginary and the corresponding discrete spectrum can be identified with that of a *gap mode* [6], i.e. of a mode whose frequency falls within the gaps in the shear Alfvén continuous spectrum. This fact can be clearly seen by taking the $(\omega/\omega_{ti}) \to \infty$ limit, for which $\Lambda = \sqrt{\omega(\omega-\omega_{*pi})}/\omega_A$. Then, the gap mode would be inside the $(0, \omega_{*pi})$ diamagnetic gap [6]. In the present case, the frequency gap structure is complicated by the inclusion of core ion compressibility effects. However, it is conceptually the same.

The continuous spectrum is obtained for purely real Λ [6]. In fact, in this case the mode eigenfunction in θ space has a purely oscillatory asymptotic behaviour and cannot be normalized: the corresponding eigenfunction in real space has logarithmic singularities for $qR_0k_\parallel = \pm\Lambda$, as it may be readily verified (cf appendix B). The modes of the Alfvén

continuum result in incoherent plasma oscillations, obtained as superposition of local (in real space) perturbations of the type [14]

$$\frac{1}{t}\exp(-\mathrm{i}\omega(r)t) \tag{22}$$

where r is a radial-like flux variable and $\omega(r)$ is obtained from the 'local dispersion relation'

$$q(r)R_0 k_\parallel(r) = \pm\Lambda(\omega(r)). \tag{23}$$

Note that $\omega(r)$, as obtained from equation (23), is generally complex since Λ is a transcendental function. This fact is remarkable since it predicts the existence of *unstable continua* for $\mathrm{Im}\,\omega(r) > 0$, which is impossible in ideal MHD. In fact, this is also impossible in kinetic MHD when only diamagnetic effects are included. The novel feature is entirely due to the inclusion of core-plasma ion compressibility in the theoretical analysis.

In order to study the various modes described by the dispersion relation, equation (21), it is useful to classify them according to the accumulation points of the continuous spectrum, which they merge into when $\delta W_f \to 0$. The accumulation points are obtained for $\Lambda = 0$, and since Λ is a transcendental function there are infinitely many of them. Thus, we will limit ourselves to consider the most unstable (least stable) ones. For simplicity, let us assume $|\omega|/\omega_{\mathrm{ti}} \gg 1$. In this case, it may be shown that

$$\frac{\Lambda^2}{\beta_{\mathrm{i}}} = \left(\Omega^2 - \frac{7}{4}q^2\right)\left(1 - \frac{\Omega_{*\mathrm{pi}}}{\Omega}\right) + \frac{7}{4}q^2\frac{\Omega_{*T_{\mathrm{i}}}}{\Omega} - q^2\frac{\left(1 - \Omega_{*\mathrm{pi}}/\Omega\right)^2}{\left(1/\tau + \Omega_{*n_{\mathrm{i}}}/\Omega\right)}$$

$$+\mathrm{i}\sqrt{\pi}q^2\,\mathrm{e}^{-\Omega^2}\left(\Omega - \Omega_{*n_{\mathrm{i}}} - \eta_{\mathrm{i}}\Omega^2\Omega_{*n_{\mathrm{i}}}\right)\left(\Omega^2 + \frac{1 - \Omega_{*\mathrm{pi}}/\Omega}{1/\tau + \Omega_{*n_{\mathrm{i}}}/\Omega}\right)^2. \tag{24}$$

Here, $\eta_{\mathrm{i}} = (\partial\ln T_{\mathrm{i}}/\partial\ln n_{\mathrm{i}})$, $\Omega = \omega/\omega_{\mathrm{ti}}$, $\Omega_{*\mathrm{pi}} = \omega_{*\mathrm{pi}}/\omega_{\mathrm{ti}}$ and the other symbols are analogously defined.

An explicit expression for the accumulation points of the continuous spectrum can be found for $\eta_{\mathrm{i}} = 0$, yielding

$$\Omega = \Omega_{*n_{\mathrm{i}}} \qquad \text{and} \qquad \Omega = \Omega_0 - \mathrm{i}\frac{\sqrt{\pi}}{2}q^2\Omega_0^4\,\mathrm{e}^{-\Omega_0^2} \tag{25}$$

where

$$\Omega_0^2 = \begin{cases} (\frac{7}{4} + \tau)q^2 & \text{for } \Omega_{*n_{\mathrm{i}}} \ll |\Omega_0| \\ \frac{3}{4}q^2 & \text{for } \Omega_{*n_{\mathrm{i}}} \gg |\Omega_0|. \end{cases} \tag{26}$$

Thus, we see that, in the $|\omega|/\omega_{\mathrm{ti}} \gg 1$ limit, three accumulation points of the continuous Alfvén spectrum may be found close to the real frequency axis. Two directly related to the beta-induced gap and one associated with the ion diamagnetic gap. Hence, in the following, we will call KBM those modes merging into the $\Omega \sim \Omega_{*\mathrm{pi}}$ accumulation point when $\delta W_f \to 0$. Similarly, the modes merging into the $\Omega^2 \sim (\frac{7}{4} + \tau)q^2$ (or $\Omega^2 \sim \frac{3}{4}q^2$) accumulation points as $\delta W_f \to 0$ will be referred to as BAE. More precisely, only the branch with $\mathrm{Re}\,\Omega > 0$ will be called BAE, since we are interested only in modes propagating in the ion diamagnetic direction (cf sections 1, 3 and appendix A).

Approximate expressions for the continuum accumulation points can also be found in the general $\eta_{\mathrm{i}} \neq 0$ case. For $\Omega_{*\mathrm{pi}}^2 \gg (\frac{7}{4} + \tau)q^2$, the KBM accumulation point turns out to be

$$\Omega = \Omega_{*\mathrm{pi}}\left[1 - \frac{7}{4}\frac{q^2}{\Omega_{*\mathrm{pi}}^2}\frac{\eta_{\mathrm{i}}}{1 + \eta_{\mathrm{i}}} + \mathrm{i}\sqrt{\pi}q^2\frac{\eta_{\mathrm{i}}}{1 + \eta_{\mathrm{i}}}\Omega_{*\mathrm{pi}}^5\,\mathrm{e}^{-\Omega_{*\mathrm{pi}}^2}\right] \tag{27}$$

whereas the BAE accumulation points are given by

$$\Omega = \Omega_0 + \frac{q^2}{\Omega_{*n_i}}\left(1 + \frac{1+\eta_i}{2\tau}\right) - \frac{q^2}{2\Omega_{*pi}}\left(\frac{1+\eta_i/4+\eta_i^2}{1+\eta_i}\right) - i\frac{\sqrt{\pi}}{2}q^2\frac{\eta_i}{1+\eta_i}\Omega_0^6\,e^{-\Omega_0^2}$$

$$\Omega_0^2 = \frac{3}{4}\frac{q^2}{1+\eta_i}\left[1 + 2\eta_i - \frac{4}{3}\eta_i^2\right]. \tag{28}$$

Note that the approximations leading to equation (28) require $\Omega_0^2 \gg 1$ (i.e. large and real). Analogously, for $\Omega_{*pi}^2 \ll (\frac{7}{4}+\tau)q^2$, we find

$$\Omega = \Omega_0 + i\frac{2}{7}\sqrt{\pi}\frac{\Omega_0^5}{\Omega_{*n_i}}(\Omega_0 + \tau\Omega_{*n_i})(\Omega_0 - \Omega_{*n_i} - \eta_i\Omega_0^2\Omega_{*n_i})$$

$$\times\left[\left(\eta_i + \frac{1+\tau}{2}\right)^2 + \frac{4}{7}\tau\eta_i(1+\eta_i+\tau)\right]^{-1/2} \tag{29}$$

$$\Omega_0 = \frac{\Omega_{*n_i}}{1+4\tau/7}\left\{\frac{4}{7}\tau(1+\eta_i) + \eta_i + \frac{1-\tau}{2} + \left[\left(\eta_i + \frac{1+\tau}{2}\right)^2 + \frac{4}{7}\tau\eta_i(1+\eta_i+\tau)\right]^{1/2}\right\}$$

for the KBM accumulation point, while those related to the beta-induced gap are given by

$$\Omega = \Omega_0 - \frac{\Omega_{*n_i}}{2\Omega_0^2}q^2\left(\frac{7}{4}\eta_i + \tau(1+\eta_i) + \tau^2\right) - i\frac{\sqrt{\pi}}{2}q^2\Omega_0^4\,e^{-\Omega_0^2}\left(1 - \eta_i\Omega_0\Omega_{*n_i}\right) \tag{30}$$

$$\Omega_0^2 = \left(\frac{7}{4}+\tau\right)q^2.$$

Equations (27) and (28) refer to the situation in which the core-plasma dynamics is dominated by ion diamagnetic effects and core-plasma ion compressibility may be ignored. Hence, it is not surprising that the highest frequency accumulation point is close to that of the well known ion diamagnetic frequency gap, $(0, \omega_{*pi})$. Equations (29) and (30), meanwhile, correspond to the case where diamagnetic effects are small with respect to core-plasma compressibility [3, 4]. The highest frequency accumulation points of the Alfvén continuum, $\Omega^2 \sim (\frac{7}{4}+\tau)q^2$, are now those related to the beta-induced Alfvén gap. This is the limiting case we must refer to in order to establish a bridge between the present kinetic theory and previous theoretical analyses [3, 4], based on ideal MHD, which predict the accumulation points of the beta-induced Alfvén gap at $\Omega^2 = \gamma q^2$, where γ is the ratio of specific heats.

The next section is devoted to numerical studies of the dispersion relation, equation (21), to point out the peculiarities of both BAE and KBM modes and to clarify the strong relation existing between these two branches. However, before proceeding further, it is worthwhile analysing the conditions under which the accumulation points of the continuous spectrum, mentioned so far, may be located in the upper half complex Ω plane, i.e. may become unstable. From a direct check of equations (29) and (30) it is readily verified that the KBM accumulation point is always stable for $\Omega_{*pi}^2 \ll (7/4+\tau)q^2$. This is not the case for the BAE accumulation point (that with $\mathrm{Re}\,\Omega > 0$). In fact, it may become unstable for η_i larger than a critical value η_{ic}, given by

$$\eta_{ic}\Omega\Omega_{*n_i} \simeq 1 \qquad \Rightarrow \eta_{ic} \simeq \frac{2}{\sqrt{7+4\tau}}\frac{\omega_{ti}}{q\omega_{*n_i}}. \tag{31}$$

Equation (31) can be interpreted as the threshold condition for the onset of an unstable continuous spectrum. Note that the threshold is only an estimate, although it should give the correct scaling with equilibrium parameters. For $\Omega_{*pi}^2 \gg (\frac{7}{4}+\tau)q^2$, equation (27) predicts the KBM accumulation point to be unstable, although $\mathrm{Im}(\Omega)$ is expected to

be exponentially small compared with that obtained from equation (30) for $\eta_i > \eta_{ic}$. Meanwhile, equation (28) shows that the BAE accumulation point is always stable for $\Omega^2_{*pi} \gg (\frac{7}{4} + \tau)q^2$.

From the previous analysis we get a qualitative picture of the Alfvén spectra described by the dispersion relation equation (21). When $\Omega^2_{*pi} \ll (\frac{7}{4} + \tau)q^2$, only the BAE accumulation point may be unstable for $\eta_i > \eta_{ic}$, with $\text{Im}(\Omega)$ increasing linearly with η_i and Ω_{*n_i}. If Ω_{*pi} is further increased, the unstable BAE accumulation point is expected to smoothly connect to an unstable KBM accumulation point, with exponentially small $\text{Im}(\Omega)$ when $\Omega^2_{*pi} \gg (\frac{7}{4} + \tau)q^2$. This fact allows us to anticipate a result of the next section; i.e. that the most unstable BAE/KBM accumulation point occurs at $\Omega^2_{*pi} \approx (\frac{7}{4} + \tau)q^2$, when BAE and KBM branches are strongly coupled.

6. Numerical studies of the dispersion relation

In the numerical studies of the dispersion relation, equation (21), we focus our attention on the 'gap mode' for both BAE and KBM branches, and on the 'local frequencies' associated with the continuous spectrum. We believe that these analyses are sufficient to exhaustively illustrate the relevant aspects of the low-frequency Alfvén spectrum. Theoretical studies of the 'energetic particle continuum modes' [6] for the BAE and KBM branches will be presented in a future work. Detailed numerical simulations of energetic particle excitations of KBMs in tokamak plasmas are presented in [15].
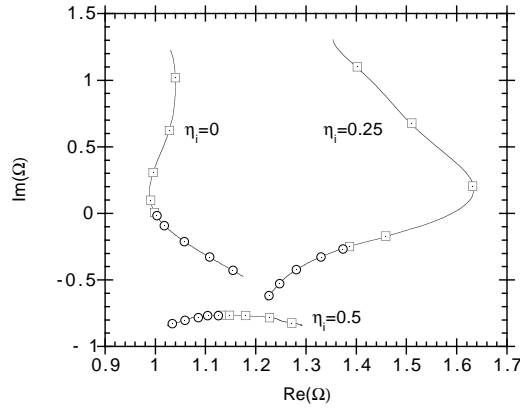
The numerical results, presented in the following, assume $\beta_i = 0.01$, $\tau = T_e/T_i = 1$ and $q = 1.5$. These parameters are kept fixed and are considered to be representative of a typical tokamak local plasma equilibrium. In figure 1, the BAE spectrum is shown for $\Omega_{*n_i} = 1$. The three curves which are shown are characterized by different values of η_i. The branches marked with open squares correspond to δW_f ranging in the interval $(-0.2, 0)$, i.e. to the BAE gap mode. Open circles refer to the solution of equation (23), with $q(r)R_0k_\parallel(r)$ varying between $(0, 0.2)$, i.e. to the continuous spectrum. The accumulation points of the Alfvén continuum are visible as the positions where the gap mode merges into the continuous spectrum, i.e. where open squares and open circles overlap. Figure 2 shows the same parametric studies reported in figure 1, but focused on the KBM branch. For completeness, in figure 3 we also report the analysis of the branch propagating in the electron diamagnetic direction, which confirms that it does not exhibit interesting features. For this reason and for those discussed in appendix A, we shall neglect it in the following.

A direct comparison of figure 1 and figure 2 shows how the frequency spectra qualitatively change with η_i. More specifically, the $\eta_i = 0.5$ case differs from the others, since it is characterized by unstable BAE and stable KBM gap modes. Furthermore, the Alfvén continuum associated with the BAE accumulation point is clearly unstable. This fact confirms the existence of unstable continua above a critical η_{ic} and indicates that this phenomenon is deeply connected with a strong coupling between BAE and KBM modes. Figure 4 shows this point more clearly. The four curves are all obtained for δW_f ranging in the interval $(-0.14, -0.06)$. Open squares refer to the KBM branch, whereas open circles indicate BAE gap modes. The coupling between the two branches is evident and it indicates a value of η_{ic} in the interval $(0.25, 0.28)$; consistent with the prediction of equation (31).

Figures 5 and 6 show the same parametric studies and use the same conventions of figures 1 and 2, except that here $\Omega_{*n_i} = 0.5$. The same considerations which were made in the previous case hold here. In contrast, figures 7 and 8, where $\Omega_{*n_i} = 3$, exhibit new qualitative features of the BAE/KBM spectra. First of all, the BAE branch never becomes
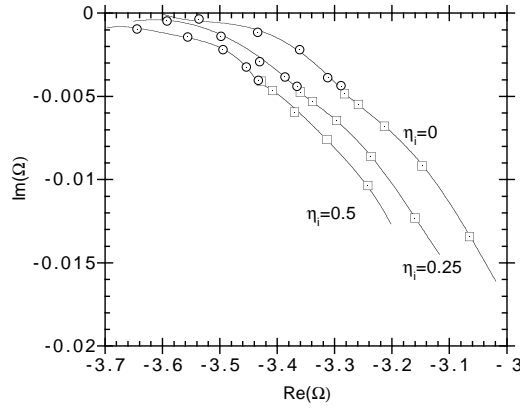
Figure 1. The BAE branch is shown for $\beta_i = 0.01$, $\tau = 1$, $q = 1.5$ and $\Omega_{*n_i} = 1$. The BAE spectrum is reported for three values of $\eta_i = 0, 0.25, 0.5$. Open squares refer to the gap mode $\delta W_f \in (-0.2, 0)$; open circles indicate the continuum $q(r)R_0 k_\parallel(r) \in (0, 0.2)$.
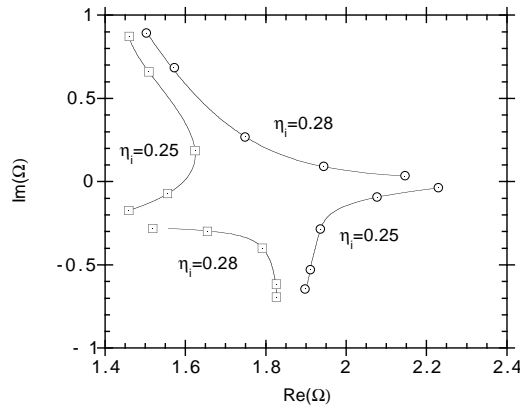

Figure 2. The KBM branch is shown for the same parametric studies reported in figure 1.

unstable; second, even if a value for η_i can still be identified (between 0.5 and 1), above which BAE and KBM strongly couple, this value can no longer be considered as a threshold for the continuous spectrum to be unstable. In fact, ImΩ at the most unstable (that of KBM) accumulation point is exponentially small, as predicted by equation (27). The difference with respect to the previous cases is entirely due to the value of Ω_{*n_i}. For $\Omega_{*pi} < \sqrt{\frac{7}{4} + \tau} \, q$, the features of the BAE/KBM spectrum are those of figures 1, 2 and 5, 6. The dominant modes for $\eta_i > \eta_{ic}$ are those of the BAE branch, and in this case part of the continuous Alfvén spectrum is unstable. In the $\Omega_{*pi} > \sqrt{\frac{7}{4} + \tau} \, q$ case, however, the features of the BAE/KBM spectrum are those of figures 7 and 8. The dominant modes are of the KBM branch and the Alfvén continuum is always stable (it coincides with that predicted in ideal MHD with diamagnetic effects included). The present discussion is consistent with the statement, made in the previous section, that the KBM accumulation point has an exponentially small ImΩ for $\Omega_{*pi} > \sqrt{\frac{7}{4} + \tau} \, q$.
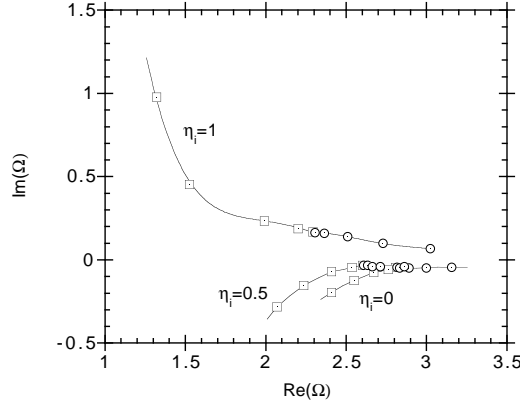
Figure 3. The branch propagating in the electron diamagnetic drift direction is shown for the same parametric studies reported in figure 1.
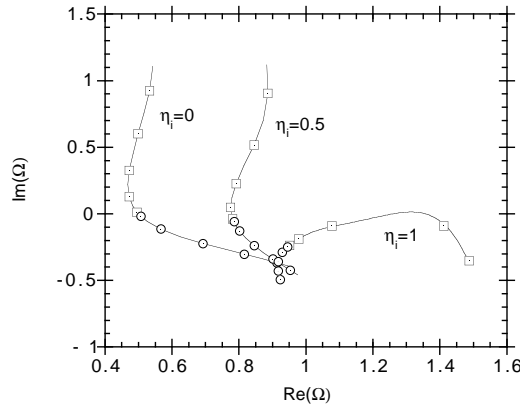

Figure 4. Two spectra with $\eta_i = 0.25$ and $\eta_i = 0.28$ illustrate the coupling of BAE (open circles) and KBM (open squares) branches. $\delta W_f \in (-0.14, -0.06)$ in all cases. Equilibrium parameters are those of figure 1.

For $\Omega_{*pi} \approx \sqrt{\frac{7}{4} + \tau}\, q$, BAE and KBM branches are strongly coupled. In the previous section, it was anticipated that in this parameter range $\mathrm{Im}\,\Omega$ of the unstable BAE/KBM accumulation point is expected to be peaked. This aspect is examined in figures 9 and 10, where imaginary and real parts of the BAE/KBM accumulation point are respectively shown against Ω_{*n_i} and for different values of η_i. Open circles refer to the $\eta_i = 0.5$ case, open squares to $\eta_i = 1.0$ and open triangles to $\eta_i = 1.5$. For $\Omega_{*pi} \ll \sqrt{\frac{7}{4} + \tau}\, q$, the numerical results are well described by the analytical estimate, equation (30), indicating that the unstable accumulation point is of BAE type (note that $\eta_i > \eta_{ic}$). In fact, $\mathrm{Im}\,\Omega$ increases linearly with both Ω_{*n_i} and η_i, whereas $\mathrm{Re}\,\Omega$ linearly decreases. When $\Omega_{*pi} \approx \sqrt{\frac{7}{4} + \tau}\, q$, the strong coupling of BAE with KBM results in the break down of equation (30): $\mathrm{Re}\,\Omega$ begins to increase and the behaviour of $\mathrm{Im}\,\Omega$ is no longer linear. Finally, the dependence of the unstable accumulation point on Ω_{*n_i} and η_i becomes of KBM type for $\Omega_{*pi} \gg \sqrt{\frac{7}{4} + \tau}\, q$, as predicted by equation (27). Thus, figures 9 and 10 illustrate the smooth transition from

Figure 5. The BAE branch is shown for $\beta_i = 0.01$, $\tau = 1$, $q = 1.5$ and $\Omega_{*n_i} = 0.5$. The BAE spectrum is reported for three values of $\eta_i = 0, 0.5, 1$. Open squares refer to the gap mode $\delta W_f \in (-0.2, 0)$; open circles indicate the continuum $q(r)R_0 k_\parallel(r) \in (0, 0.2)$.
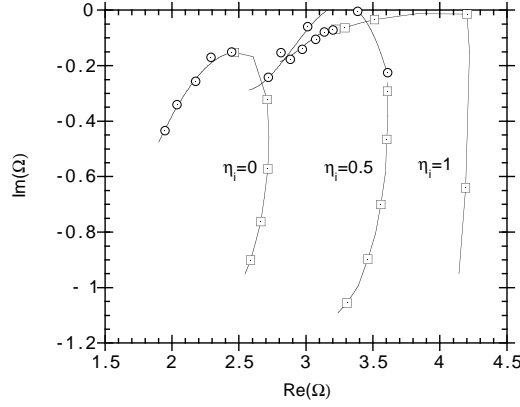

Figure 6. The KBM branch is shown for the same parametric studies reported in figure 5.
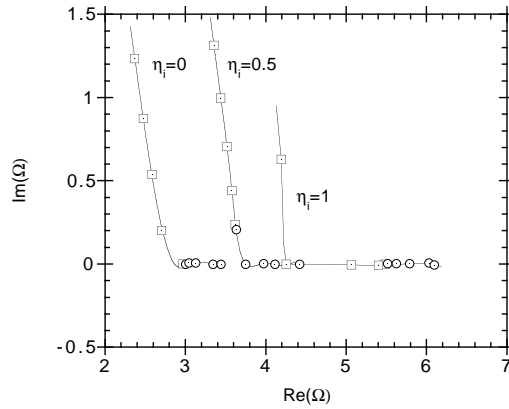
an unstable BAE to an unstable KBM branch, passing through a situation characterized by a spectrum of modes with a mixed BAE/KBM nature. This situation, occurring for $\Omega_{*pi} \gtrsim \sqrt{\frac{7}{4} + \tau} \, q$, corresponds to the most unstable regime, as anticipated in the previous section.

7. Conclusions and discussions

In the present work, we have discussed a comprehensive kinetic theory of high toroidal mode number low-frequency ($\omega \approx \omega_{*pi} \approx \omega_{ti}$) Alfvén waves in a high-β tokamak equilibrium. By including diamagnetic effects and finite core-plasma ion compressibility on the same footing, we have generalized the KBM theory of Tsai and Chen [6], and have discussed the important relationship which generally exists between BAE and KBM spectra. BAE and KBM are *separate* branches of the low-frequency shear Alfvén spectrum, which are independent only at $\eta_i = 0$. In fact, they are coupled in the general $\eta_i \neq 0$ case.
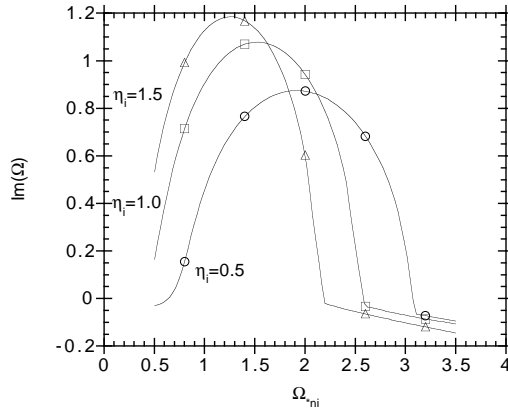
Figure 7. The BAE branch is shown for $\beta_i = 0.01$, $\tau = 1$, $q = 1.5$ and $\Omega_{*n_i} = 3$. The BAE spectrum is reported for three values of $\eta_i = 0, 0.5, 1$. Open squares refer to the gap mode $\delta W_f \in (-0.2, 0)$; open circles indicate the continuum $q(r) R_0 k_\parallel(r) \in (0, 0.2)$.
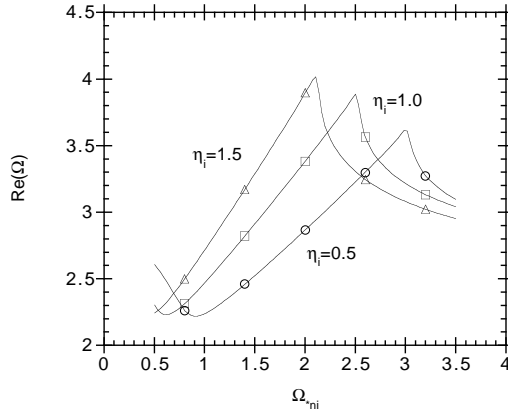

Figure 8. The KBM branch is shown for the same parametric studies reported in figure 7.

It has been shown that the theory of [6] applies for $\omega_{*pi} \gg \sqrt{\frac{7}{4} + \tau} q \omega_{ti}$, as expected, a condition under which KBM are the most unstable modes of those considered here. More importantly, we have demonstrated that, for $\omega_{*pi} < \sqrt{\frac{7}{4} + \tau} q \omega_{ti}$, a critical value η_{ic} exists, above which the BAE mode is the most unstable branch, thereby showing that BAEs are not always Landau damped as simple considerations based on its frequency would suggest [16]. It has also been shown that, for $\eta_i > \eta_{ic}$, part of the continuous Alfvén spectrum may be unstable. This implies that non-collective modes may be present in the plasma, formed as a superposition of local oscillations which are quasi-exponentially growing in time. This new feature is entirely due to the inclusion of finite core-plasma ion compressibility in the theoretical analysis. Finally, it has been shown that the most unstable low-frequency Alfvén modes occur at $\omega_{*pi} \gtrsim \sqrt{\frac{7}{4} + \tau} q \omega_{ti}$, corresponding to a parameter range in which BAE and KBM are strongly coupled.

The present theory of BAE/KBM linear stability yields an analytic expression of the mode dispersion relation, which may be generalized to include resonant wave excitations

Figure 9. Im(Ω) of the most unstable BAE/KBM accumulation point is shown against Ω_{*n_i} for $\beta_i = 0.01$, $\tau = 1$, $q = 1.5$, $\delta W_f = 0$ and different values of η_i: $\eta_i = 0.5$ (open circles), $\eta_i = 1.0$ (open squares) and $\eta_i = 1.5$ (open triangles).

Figure 10. Re (Ω) of the most unstable BAE/KBM accumulation point is shown against Ω_{*n_i} for the same parameters of figure 9.

by energetic particles with finite orbit widths [6]. It has been shown that, in general, two types of spectra may exist: a discrete spectrum of gap modes, which is present only when the tokamak plasma is ideal MHD unstable; and the Alfvén continuous spectrum, which may be characterized, under certain conditions, by unstable accumulation points.

The issue of energetic particle continuum modes [6], which may also exist for $\delta W_f > 0$, but require that the energetic particle drive be strong enough to overcome continuum damping, is not analysed here. The numerical studies of the analytic dispersion relation deal only with BAE/KBM gap modes and with the Alfvén continuous spectrum. Finally, it is clear that the present theoretical results may have important implications for the stability and transport properties of tokamak experiments with and without energetic particles. Further theoretical delineations and comparisons with experimental results are, however, beyond the scope intended for this work and will be discussed in future publications.

Acknowledgments

Appendix A. Validity of the ideal MHD limit $\delta E_\parallel = 0$

At order $O(\beta)$, the quasi-neutrality equation, equation (5), becomes

$$\left(\frac{1}{\tau} + \frac{\omega_{*n_i}}{\omega}\right)(\delta\Phi^{(0)} - \delta\Psi^{(0)}) + \left(1 - \frac{\omega_{*pi}}{\omega}\right)b_i\delta\Psi^{(0)} = \frac{T_i k_\perp}{n e k_\vartheta}\left\langle -\frac{k_\perp^2\rho_{Li}^2}{4}\delta K_i^{(0)} + \delta K_i^{(2)}\right\rangle.$$

(A1)

Here, $\delta K_i^{(2)}$ is obtained from

$$(\omega_{tr}\partial_{\theta_0} - i\omega)\delta K_i^{(2)} = -(\omega_{tr}\partial_{\theta_1} + i\omega_{di})\delta K_i^{(1)} + i\left(\frac{e k_\vartheta}{m_i k_\perp}\right)$$

$$\times Q F_{0i}\left[(\delta\Phi^{(2)} - \delta\Psi^{(2)}) - \frac{k_\perp^2\rho_{Li}^2}{4}(\delta\Phi^{(0)} - \delta\Psi^{(0)}) + \frac{m_i v_\perp^2}{2eB}\delta\hat{B}_\parallel^{(0)}\right].$$

(A2)

In order to get from equation (A1) an expression for $(\delta\Phi^{(0)} - \delta\Psi^{(0)})$ valid up to $O(\beta)$, we need to solve equation (A2) just for $\overline{\delta K_i^{(2)}}$, where $\overline{[...]} = (1/2\pi)\oint(...)\,d\theta_0$. It is possible to show that

$$\overline{\delta K_i^{(2)}} = \left(\frac{e k_\vartheta}{m_i k_\perp}\right)\frac{Q F_{0i}}{\omega}\left[\frac{k_\perp^2\rho_{Li}^2}{4}(\delta\Phi^{(0)} - \delta\Psi^{(0)}) - \frac{m_i v_\perp^2}{2eB}\delta\hat{B}_\parallel^{(0)}\right] - i\frac{\omega_{tr}}{\omega}\partial_{\theta_1}\overline{\delta K_i^{(1)}} + \frac{\overline{\omega_{di}}}{\omega}\delta K_i^{(1)}.$$

(A3)

When substituted into equation (A1), equation (A3) yields the $O(\beta)$ quasi-neutrality condition, reported in section 3:

$$\frac{\omega_{ti}^2}{2\omega^2}\left(1 - \frac{\omega_{*pi}}{\omega}\right)\frac{k_\perp}{k_\vartheta}\frac{\partial^2}{\partial\theta_1^2}\left[\frac{k_\vartheta}{k_\perp}(\delta\Phi^{(0)} - \delta\Psi^{(0)})\right] + \left(\frac{1}{\tau} + \frac{\omega_{*n_i}}{\omega}\right)(\delta\Phi^{(0)} - \delta\Psi^{(0)})$$

$$+ \left\{\left(1 - \frac{\omega_{*pi}}{\omega}\right)b_i + q^2 b_i\frac{\omega_{ti}}{\omega}\left[\left(1 - \frac{\omega_{*n_i}}{\omega}\right)F(\omega/\omega_{ti})\right.\right.$$

$$\left.\left. - \frac{\omega_{*T_i}}{\omega}G(\omega/\omega_{ti}) - \frac{N^2(\omega/\omega_{ti})}{D(\omega/\omega_{ti})}\right]\right\}\delta\Phi^{(0)}$$

$$= \frac{b_i^{1/2}\alpha}{2^{3/2}q}\frac{\omega_{ti}}{\omega}\frac{k_\vartheta}{k_\perp}\left(1 - \frac{\omega_{*pi}}{\omega}\right)\delta\Psi^{(0)}.$$

(A4)

Equation (A4) demonstrates that $(\delta\Phi^{(0)} - \delta\Psi^{(0)}) = O(\beta)$, i.e. $\delta E_\parallel \simeq 0$, for long wavelength modes ($\partial_{\theta_1} = O(\beta^{1/2})$) with $\omega_{*pi}/\omega = O(1)$ and which propagate in the ion diamagnetic direction ($(1/\tau + \omega_{*n_i}/\omega) = O(1)$). In the present paper, we refer to this type of mode.

For waves which propagate in the electron diamagnetic direction, equation (A4) predicts that an appreciable parallel electric field can be originated for $(1/\tau + \omega_{*n_i}/\omega) = O(b_i)$. Another possibility for the $\delta E_\parallel \simeq 0$ assumption to break down is $\omega_{*pi}/\omega = O(1/\beta)$. These modes would interact strongly with the long wavelength slab-like ion temperature gradient (ITG) driven mode [7–9] and are out of the scope of the present analysis.

Equation (A4) serves also to the scope of discussing the validity of the $\delta E_\parallel = 0$ assumption at moderate $|\theta|$ values. In fact, for $|\theta| < O(\beta^{-1/2})$ finite b_i and ω_{di}/ω effects may be neglected, indicating that the scale of variation of $(\delta\Phi^{(0)} - \delta\Psi^{(0)})$ is a constant. This can be also seen from a direct examination of equations (2) and (5). Moreover, since the large $|\theta|$ structure of the modes we are analysing is characterized by a long scale of variation, we must also have $\partial_\theta = $ constant $= O(\beta^{1/2})$ when acting on $(\delta\Phi^{(0)} - \delta\Psi^{(0)})$ for $|\theta| < O(\beta^{-1/2})$. Recalling that $(1/\tau + \omega_{*n_i}/\omega)$ and ω_{*pi}/ω are $O(1)$ in our analysis, the present argument and equation (A4) indicate that $\delta E_\parallel = 0$ to lowest order also for moderate $|\theta|$ values, i.e. $(\delta\Phi^{(0)} - \delta\Psi^{(0)}) = 0$. The fact that $\partial_\theta = O(\beta^{1/2})$ when acting on $(\delta\Phi^{(0)} - \delta\Psi^{(0)})$ does not indicate that the functions $\delta\Phi^{(0)}$ and $\delta\Psi^{(0)}$ vary on the long scale θ_1 only, but simply that any short-scale variation of $\delta\Phi^{(0)}$ is balanced by the same variation of $\delta\Psi^{(0)}$.

The previous discussion demonstrates that the $(\delta\Phi^{(0)} - \delta\Psi^{(0)}) = 0$ assumption also holds in the moderate $|\theta|$ region, where $\delta\Psi^{(0)}$ does not have a two-scale structure, as pointed out in section 3.2, and, in general, $\partial_\theta = O(1)$ due to finite (s, α) effects, as it emerges from equation (15).

Appendix B. Logarithmic singularities and continuous spectrum

A simple derivation of equation (23) can be obtained transforming the ballooning eigenfunction $\delta\psi(\theta) = [k_\vartheta/k_\perp(\theta)]\delta\Psi(\theta)$ back to real space [17]

$$\widehat{\delta\psi}(nq - m) = \int_{-\infty}^{+\infty} \frac{\delta\Psi(\theta)\exp[-i(nq - m)\theta]}{[1 + (s\theta - \alpha\sin\theta)^2]^{1/2}}\,d\theta. \tag{B1}$$

From equation (B1), it is easily shown that

$$\frac{is\partial\widehat{\delta\psi}(nq - m)}{\partial(nq - m)} = \int_{-\infty}^{+\infty} \frac{s\theta\delta\Psi(\theta)\exp[-i(nq - m)\theta]}{[1 + (s\theta - \alpha\sin\theta)^2]^{1/2}}\,d\theta. \tag{B2}$$

Define, now, a value Θ such that $\Theta \gg 1$ and $\beta^{1/2}\Theta \ll 1$. In this way, the integration interval in equation (B2) can be subdivided into $[-\Theta, \Theta]$, where the 'ideal' solution $\delta\Psi_{ID}$ can be used, and $(-\infty, -\Theta] \cup [\Theta, +\infty)$, where the 'inertial layer' solution $\delta\Psi_{IN}$ is appropriate. With the explicit use of equation (18), it is possible to show

$$\frac{is\partial\,\widehat{\delta\psi}(nq - m)}{\partial(nq - m)} = \int_{-\Theta}^{\Theta} \frac{s\theta\delta\Psi_{ID}(\theta)\exp[-i(nq - m)\theta]}{[1 + (s\theta - \alpha\sin\theta)^2]^{1/2}}\,d\theta$$

$$+ \int_{\Theta}^{\infty} [\exp i(m - nq)\theta - \exp i(nq - m)\theta]\,e^{i\Lambda\theta}\,d\theta$$

$$+ O\left(\frac{1}{s^2\Theta^2}\right) + O\left(\frac{\alpha}{s\Theta}\right) + O\left(\frac{1}{\Theta}\right). \tag{B3}$$

Since the contribution from the $[-\Theta, \Theta]$ integral is typically $O(\Theta)$, whereas that from the $[\Theta, \infty)$ interval is $O(\beta^{-1/2})$ for $|nq - m| = O(\beta^{1/2})$, equation (B3) implies

$$\frac{s\partial\,\widehat{\delta\psi}(nq - m)}{\partial(nq - m)} = \left[\frac{\exp i\Theta(m - nq)}{\Lambda - (nq - m)} - \frac{\exp i\Theta(nq - m)}{\Lambda + (nq - m)}\right]e^{i\Lambda\Theta} + O\left(\frac{1}{s^2\Theta^2}\right)$$

$$+ O\left(\frac{\alpha}{s\Theta}\right) + O\left(\frac{1}{\Theta}\right) + O(\beta^{1/2}\Theta). \tag{B4}$$

Equation (B4) is readily integrated and yields

$$\widehat{\delta\psi}(nq - m) = C - \frac{1}{s}\ln[\Lambda^2 - (nq - m)^2] \tag{B5}$$

for $|nq - m| \approx |\Lambda| = \mathrm{O}(\beta^{1/2})$, where C is an integration constant and $\mathrm{O}(\beta^{1/2}\Theta)$ terms have been consistently neglected. Equation (B5) indicates that the wave field in real space has a logarithmic singularity when $(nq - m) = \pm\Lambda$, i.e. when

$$q(r)R_0 k_\parallel(r) = \pm\Lambda(\omega(r))$$

which is equation (23). In an initial-value analysis, the just derived logarithmic singularity becomes a logarithmic branch point in the complex omega plane. When the time asymptotic behaviour is computed, the finite jump of the wave field across the branch cut, originating from the logarithmic branch point, gives the contribution

$$\frac{1}{t}\exp(-\mathrm{i}\omega(r)t)$$

of equation (22). A detailed analysis, yielding to this result, can be found in [14]. Here, we just wish to note that the concepts of continuous spectrum, satisfying equation (23), and of singular local plasma oscillations are closely related.

References

[1] Heidbrink W W, Strait E J, Chu M S and Turnbull A D 1993 *Phys. Rev. Lett.* **71** 855
[2] Cheng C Z, Chen L, Chance M S 1985 *Ann. Phys.* **161** 21
[3] Turnbull A D, Strait E J, Heidbrink W W, Chu M S, Greene J M, Lao L L, Taylor T S and Thompson S J 1993 *Phys. Fluids* B **5** 2546
[4] Chu M S, Greene J M, Lao L L, Turnbull A D and Chance M S 1992 *Phys. Fluids* B **4** 3713
[5] Biglari H and Chen L 1991 *Phys. Rev. Lett.* **67** 3681
[6] Tsai S T and Chen L 1993 *Phys. Fluids* B **5** 3284
[7] Chen L, Briguglio S and Romanelli F 1991 *Phys. Fluids* B **3** 611
[8] Romanelli F, Chen L and Briguglio S 1991 *Phys. Fluids* B **3** 2496
[9] Guo S C and Romanelli F 1994 *Phys. Plasmas* **1** 1101
[10] Connor J W, Hastie R J and Taylor J B 1978 *Phys. Rev. Lett.* **40** 396
[11] Antonsen T M and Lane B 1980 *Phys. Fluids* **23** 1205
[12] Chen L and Hasegawa A 1991 *J. Geophys. Res.* **96** 1503
[13] Romanelli F and Chen L 1991 *Phys. Fluids* B **3** 329
[14] Sedlàček Z 1971 *J. Plas. Phys.* **5** 239
[15] Santoro R A and Chen L 1996 *Phys. Plasmas* **3** 2349
[16] Betti R, Berk H L and Freidberg J P 1994 *Bull. Am. Phys. Soc.* **39** 1702
[17] Zonca F and Chen L 1993 *Phys. Fluids* B **5** 3668